ELSEVIER

Journal of Molecular Catalysis A: Chemical 119 (1997) 275–287

JOURNAL OF MOLECULAR CATALYSIS A: CHEMICAL

Thermodynamic and ab initio calculations of properties of chemisorbed ions and application to adsorbed sulfur oxide anions

P. Paredes Olivera [a,1], E.M. Patrito [a,1], Harrell Sellers [a,*], Evgeny Shustorovich [b]

[a] *Department of Chemistry and Biochemistry, South Dakota State University, Brookings, SD 57007, USA*
[b] *American Scientific Materials Technologies Inc., 485 Madison Avenue, 24th Floor, New York, NY 10022, USA*

Received 4 June 1996; accepted 27 September 1996

Abstract

We discuss thermodynamic conditions for the chemisorption of ions and show that, in the low coverage limit, chemisorbed cationic and anionic specie having the same stoichiometric formulas produce surface adsorbates that are virtually indistinguishable from each other and from the chemisorbed neutral species. This is also observed from high quality ab initio (RECP HF + correlation) calculations of small ions chemisorbed on silver surfaces including H^+, H^-, OH^+, OH^-, SO_3^{2-} and SO_4^{2-}. The additional demand on the cluster model of the surface in ab initio calculations due to the charge of the ion is investigated. For ionic adsorbates bigger clusters are required than in the case of neutral adsorbates. The structure of adsorbed sulfate was optimized at the Hartree–Fock level and the geometry changes upon chemisorption were found to be consistent with the principle of bond order conservation. The nature of the chemisorbed ions is discussed together with the implications that this has in the modeling of surface reactions and, in particular, in the chemistry of sulfur oxides on metal surfaces.

Keywords: Adsorption; Sulfur oxide; Thermodynamics

1. Introduction

The adsorption of ions at electrochemical interfaces is a field under active investigation [1–27]. Adsorbed anions alter the charge distribution and the structure of the electrochemical interface and therefore influence the different electrochemical processes taking place. This has important implications in the field of electrocatalysis in which, for example, Wieckowski and coworkers have recently shown [1] that the oxidation rates of methanol on single crystal Pt surfaces vary by an order of magnitude between perchloric acid and sulfuric acid solutions, giving rise to an anionic effect that matches in magnitude that due to a platinum surface structure change. The voltammetry of single crystal electrodes [2] and the structures of UPD monolayers [3] are other examples of systems which are affected by the nature of the anions used in these electrochemical processes.

Therefore, it is important to understand from a theoretical standpoint, the nature of the ion–metal bonding and the nature of adsorbed ions

* Corresponding author.
[1] On leave from Facultad de Ciencias Químicas, Universidad Nacional de Córdoba, Argentina.

PII S1381-1169(96)00491-8

on metal surfaces. Relevant issues that have to be addressed in this respect are the binding energies of the ions, the geometry relaxation of the ions induced by the adsorption process and the charge transfer processes taking place towards or from the metal surface. Since adsorbate binding energies are often calculated in ab initio methods using cluster models of the metal surface, it is also desirable to investigate the convergence of binding energies with cluster size in the case of ionic adsorbates.

In the present paper we analyze the following topics: (1) We discuss the thermodynamics involved in the chemisorption of ions and show that this thermodynamic analysis allows us to extract several conclusions concerning the nature of the chemisorbed ion. The thermodynamically derived binding energies are used as reference values for comparison with the results of our quantum mechanical calculations. (2) The reliability of the binding energies determined from ab initio calculations using cluster models of the metal surface is investigated analyzing the convergence of this property with cluster size. We show that bigger clusters than in the case of neutral adsorbates are required. The convergence of binding energy with cluster size is investigated both for mono and polyatomic ions: H^+, H^- and SO_4^{2-}. (3) We optimized the geometry of sulfate on the surface and show how the geometry relaxation of the ion can be understood in terms of the bond order conservation on metal surfaces. (4) Based on the thermodynamic and ab initio results, we discuss the nature of the adsorbed ion and we outline the implications that this has in the modeling of surface reactions and in the chemistry of sulfur oxides on metal surfaces. (5) Finally, we analyze the charge transfer processes which occur for the different adsorbates.

2. Thermodynamics of ion adsorption

In this section we derive the Schottky equations [28] for the binding of an ion to a single crystal metal surface using appropriate thermodynamic cycles. We outline the approximations which the Schottky equations contain and then we obtain the exact expression for the binding energy of an ion. Finally, and due to the lack of experimental binding energies of ions on metal surfaces, we use the Schottky equations to calculate the binding energies of common ions on different metal surfaces.

In the following thermodynamic cycles, we use the proton and hydride, H^+ and H^-, as a prototype cation and anion, respectively, and the Ni(111) surface as a metal surface. The binding energy Q of the cation is the negative of the enthalpy change of the following reaction:

$$H^+(\text{gas}) + \text{Ni}(111) \rightarrow (\text{H—Ni}(111))^+$$
$$\Delta H = -Q_{H^+}$$

in which a proton in the gas phase adsorbs on a surface. This reaction can be decomposed into several reactions with the following enthalpy changes:

$$H^+(\text{gas}) + e^- \rightarrow H(\text{gas}) \quad \Delta H = -IP_H$$
$$H(\text{gas}) + \text{Ni}(111) \rightarrow \text{H—Ni}(111)$$
$$\Delta H = -Q_H$$
$$\text{H—Ni}(111) \rightarrow (\text{H—Ni}(111))^+ + e^-$$
$$\Delta H = \phi \text{ of Ni}(111)$$

IP_H and Q_H are the ionization potential and binding energy of neutral atomic hydrogen, respectively, and ϕ is the work function of the metal surface. The adsorption of a single atom on a metal surface will not change its work function in any appreciably amount and that is why the enthalpy of the last step above is just the work function of the metal. Adding up the enthalpy changes of the three steps above we obtain

$$\Delta H = -(IP_H + Q_H) + \phi \text{ of Ni}(111)$$

The binding energy of the cation is the negative of this expression. The general expression for the binding energy of a cation is

$$Q_{\text{cation}} = Q_{\text{neutral}} + IP_{\text{neutral}} - \phi \qquad (1)$$

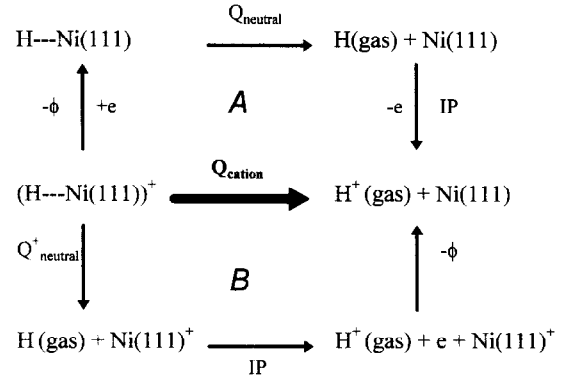

Fig. 1. Different paths along which the cation binding energy can be calculated. The bold arrow connects the initial and final states.

The steps which lead to Eq. (1) are summarized in path A of Fig. 1.A similar thermodynamic cycle for the anion is:

$$H^-(gas) \rightarrow H(gas) + e^- \quad \Delta H = -EA_H$$

$$H(gas) + Ni(111) \rightarrow H—Ni(111)$$

$$\Delta H = -Q_H$$

$$H—Ni(111) + e^- \rightarrow (H—Ni(111))^-$$

$$\Delta H = -\phi \text{ of } Ni(111)$$

EA is the electron affinity of the neutral species. The negative of the enthalpy changes of the above three reactions is the binding energy of the anion which is given by:

$$Q_{anion} = Q_{neutral} + EA_{neutral} + \phi \quad (2)$$

Eq. (1) shows that the heat of adsorption of the cation differs from that of the neutral by the difference between the ionization potential of the neutral adsorbate and the work function of the clean metal. For the anion (Eq. (2)), the heat of adsorption differs from that of the neutral by the electron affinity of the neutral and the work function of the clean metal. The relationships described by Eqs. (1) and (2) are known as the Schottky equations or Schottky barriers [28]. These equations contain the approximation that the single adsorbate has essentially no effect on the work function of the surface. However, it is possible to derive an exact expression which does not involve that approximation. We do this following path B in Fig. 1. The first step in path B corresponds to the desorption of the neutral adsorbate leaving the metal with one positive charge. The enthalpy change of this process is the binding energy of the neutral to a surface with one positive charge, $Q^+_{neutral}$. The second step is the ionization of the neutral specie with an enthalpy change given by the ionization potential IP of the neutral specie (hydrogen in Fig. 1). Finally, that electron is transferred to the surface and the enthalpy change of this process is the negative of the work function of the metal. Therefore, for the cation we have:

$$Q_{cation} = Q^+_{neutral} + IP_{neutral} - \phi \quad (3)$$

And an analogous cycle for the anion gives:

$$Q_{anion} = Q^-_{neutral} + EA_{neutral} + \phi \quad (4)$$

where $Q^-_{neutral}$ is the binding energy of the neutral specie to the infinite bulk carrying a single negative charge. No approximations are made to obtain Eqs. (3) and (4). From the comparison of Eqs. (1) and (3) for the cation and Eqs. (2) and (4) for the anion, important conclusions concerning the nature of the adsorbed species may be obtained. This point is further discussed in Section 5.

Among the parameters involved in the Schottky equations, the binding energy of the neutral is the only one which is not readily available in the literature. In the case of chlorine, its binding energy to the Pd(111) has been determined [29] which corresponds to a binding energy of 106 kcal/mol for Cl^- on Pd(111). The binding energies for hydrogen are known on several metals [30]. With these values we calculated the proton and hydride binding energies for the fcc(111) surfaces of the copper and nickel series metals in Table 1. These metals have work functions in the range of 110 to 130 kcal/mol [31]. In the case of hydrogen, the ionization potential (313 kcal/mol) is much greater than the electron affinity and greater than any of the work functions of the metals in this series. This is responsible for the fact that the hydrogen cation is more strongly bound than is the anion.

From Eqs. (1) and (2) one can calculate the

Table 1
Heats of adsorption of hydrogen cation and anion on the Cu and Ni series metals. Energies are in kcal/mol. The fcc(111) surface is assumed. The heats of adsorption of the neutral species can be found in Ref. [41] and references therein. Work functions taken from Ref. [31]

Metal	ϕ	$Q_{neutral}$	Q_{cation}	Q_{anion}
Cu	114	56	255	152
Ag	109	51	255	142
Au	122	46	237	150
Ni	123	63	253	168
Pd	129	62	246	173
Pt	131	61	243	174

shift in the binding energy upon ionization for common species such as Li^+, Na^+, K^+, F^-, Br^- and I^-. The data given in Table 2 indicate how much more or less the heat of adsorption of the ion is than the neutral. The absolute heat of adsorption of the ion can be obtained from these data if the heat of adsorption of the neutral is known. We chose silver and platinum, since they represent noble metals with a low and high work function. Since the ionization potentials of the alkali metals are close in magnitude to the work function of silver, the alkali metal cations have binding energies that are different by only 10–15 kcal/mol from the binding energies of the neutral alkali metals. The shifts in binding energies in the case of platinum are larger. In the case of platinum, the cations are less strongly bound than the neutral atoms while the halides show increases in binding energy in the range of 25–60 kcal/mol.

Table 2
Shifts in binding energy upon ionization. Energies are given in kcal/mol. The fcc(111) surface is assumed

Species	$Q_{ion} - Q_{neutral}$	
	Ag	Pt
H^+	204.0	181.6
Li^+	15.0	−7.1
Na^+	9.2	−12.9
K^+	−9.2	−31.3
F^-	29.8	51.9
Cl^-	26.0	48.1
Br^-	31.7	53.8
I^-	38.7	60.8

3. Ab initio calculations: Convergence of binding energy with cluster size

In the case of neutral specie, accurate binding energies have been obtained from ab initio calculations employing cluster models of the metal surface of modest size [32–34]. However, the situation does not have to be the same in the case of ionic adsorbates. First, the ion may transfer or accept charge from the cluster and thus it must have an adequate size to adequately describe these processes. Second, long range Coulombic interactions between the charged adsorbate and the metal also require clusters of adequate size. Therefore, in this section we investigate the convergence of binding energy with cluster size in order to (a) determine the appropriate cluster size and (b) check the reliability of the calculated binding energies. We do so for the monoatomic H^+ and H^- ions and for the polyatomic SO_4^{2-} anion. The proton and hydride were chosen as the monoatomic ions in order to compare the binding energies obtained from the ab initio calculations with those determined from the Schottky Eqs. (1) and (2).

We have performed ab initio relativistic effective core potential (RECP) Hartree–Fock + MP2 (Møller–Plesset second order perturbation theory) correlation calculations on silver clusters of various sizes that model the Ag(111) surface. The bulk silver distance of 5.45 bohr was used [31]. We employ the model potential method of Huzinaga et al. [35–37] for the description of the relativistic effective core potential metal atoms. The metal atoms are treated in two ways. At the highest level the outermost s, p, and d electrons of the atoms are included in the calculation as live quantum mechanical electrons with the remainder of the atomic electron density described by the relativistic effective core potential. At this level of theory silver atoms have eleven quantum mechanical electrons. A lower level description is available in which only a single outer s electron of the metal atom is retained as a quantum mechanical electron. In the primary chemisorption site we al-

ways employed 11-electron metal atoms and the one electron metal atoms were used only outside the primary chemisorption site. The basis sets we employed for the eleven electron silver atoms are (10s 1p 4d/3s 1p 2d) RECP basis sets. The contraction coefficients were obtained by fitting to the atomic orbitals and orbital energies as obtained from relativistic Hartree–Fock calculations in which the Darwin and mass-velocity corrections are taken into account. The sulfur and oxygen basis sets employed are (11s 7p 1d/6s 4p 1d) and (11s 7p/4s 2p) basis sets, respectively. The inclusion of d functions on sulfur is significantly more important in the calculations than the d functions on oxygen [38]. For the hydrogen ions a double-zeta basis proved to be adequate. The binding energies are defined to be the energy of the adsorbate-cluster complex minus the energies of the bare cluster and the adsorbate. Other details of the calculations such as, for example, cluster preparation are given in [38].

For the hydrogen ions, the 34 metal atom cluster of Fig. 2 was big enough. This cluster has 12 atoms in the first layer, 10 in the second and 12 in the third layer. For the three metal atoms which constitute the primary chemisorption site in the first layer and the atom below in the second layer, 11 electron silver atoms were used. The other atoms were represented by 1 electron atoms. For the sulfur oxides such as sulfate, bigger clusters were required before convergence of binding energy was achieved. Fig. 3 shows side and top views of a 52 cluster with a sulfate in a non-eclipsed coordination in which its bottom oxygens are in between metal atoms. The six metal atoms in the primary chemisorption site are 11 electron atoms while the rest are 1 electron silver atoms.

Table 3a, b contain the proton and hydride binding energies on clusters of different size. In the table we include both the SCF and total (SCF + MP2) binding energies. For the proton, the SCF binding energies range from about 230 to 250 kcal/mol which compares well with the thermodynamic value of 255 kcal/mol. The

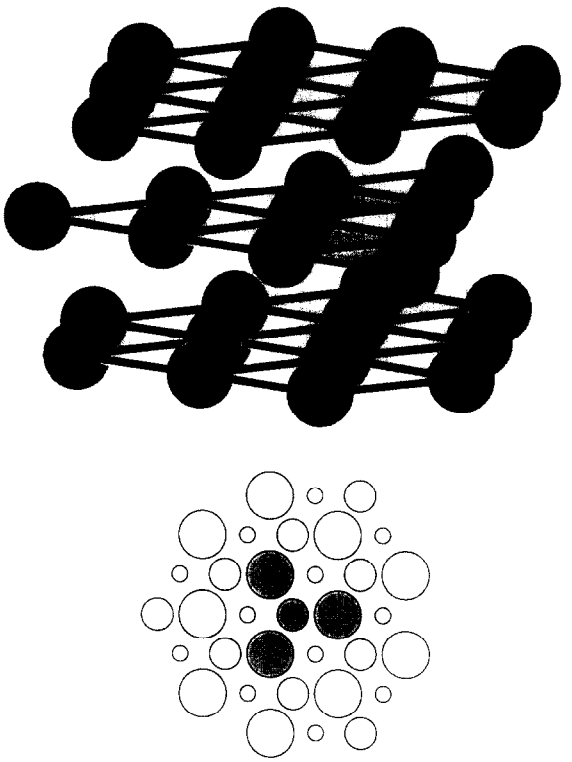

Fig. 2. Side and top views of a 34 metal atom cluster. The shaded atoms in the top view are 11 RECP electron silver atoms while the rest are 1 electron atoms.

correlation contribution to the heat of adsorption of the cation is very small and is slightly negative, indicating a little more correlation in the bare cluster than in the adsorbate-cluster complex. This is reasonable, since the same number of electrons are delocalized over more nuclei in the adsorbate-cluster complex than in the cluster.

As one might expect, in the case of the anion the influence of the size of the cluster is more pronounced. The smallest two-layer clusters yield around 80–85 kcal/mol at the RECP Hartree–Fock level for the binding energy with the larger two-layer clusters approaching 110 kcal/mol. The correlation contribution to the binding energies was in the 5–15 kcal/mol range at the MP2 level. The effect of the third layer is particularly significant in the case of the hydride. The largest three-layer clusters gave 124–130 kcal/mol at the Hartree–Fock level

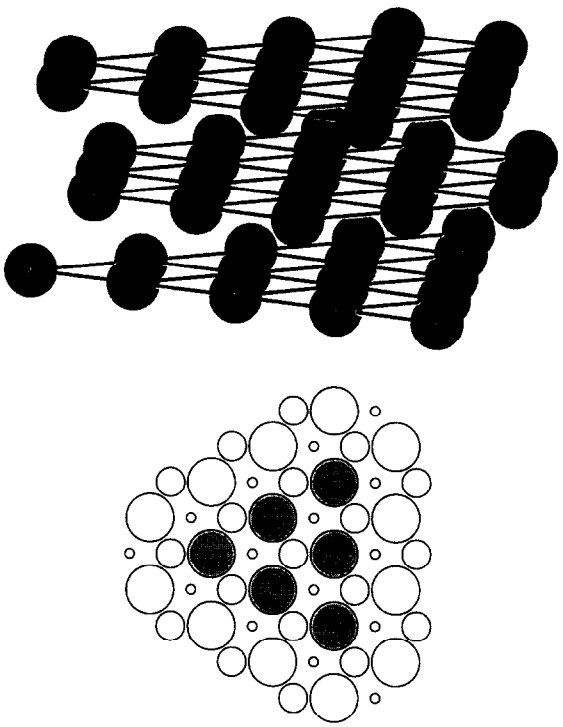

Fig. 3. Side and top views of a 52 metal atom cluster. There are six 11 RECP electron silver atoms in the first layer as indicated by the shaded atoms in the top view.

for the anion binding energy. For these larger clusters the correlation energy could not be calculated since the MP2 expansion did not converge. If the MP2 correlation contribution of about 10 kcal/mol obtained from the smaller clusters is added to the SCF binding energies of the bigger clusters (124–130 kcal/mol), we obtain a hydride binding energy of 134–140 kcal/mol which compares very well with the thermodynamic value of 142 kcal/mol.

Table 3
Proton and hydride binding energies calculated at different levels of theory on clusters of different size

Cluster	H^+			H^-		
	SCF	MP2	total	SCF	MP2	total
4 (3, 1)	261	−11	250	85	15	100
10 (7, 3)	240	−11	229	83	5	88
16 (7, 6, 3)	245	2	247	124	3	127
34 (12, 10, 12)	249	−5	244	130	—	
82 (21, 19, 21, 21)	245	—	—	124	—	
Thermodynamic value	255	255	255	142	142	142

Table 4
Sulfate binding energies calculated on clusters of different size with (A) four 11 RECP electron silver atoms in the primary chemisorption site and (B) six 11 RECP electron atoms in the primary chemisorption site

		HF	MP2	total
A	22 (12/10)	90.9	14.5	105.4
	28 (12/10/6)	93.4	25.0	118.4
	34 (12/10/12)	99.4	24.7	124.1
	40 (18/10/12)	107.2	25.6	132.8
	52 (18/19/15)	136		
	64 (27/25/12)	133.1		
B	28 (12/10/6)	93.4		
	52 (18/19/15)	121.7		

In the case of sulfate, since it is a much bigger adsorbate, we investigated the convergence of the binding energy both with the cluster size and the number of 11 RECP electron silver atoms in the primary chemisorption site. Table 4 contains the binding energies for clusters of different size. All these clusters have three 11 electron silver atoms in the first layer and one in the second layer. In going from the cluster with 22 atoms to the cluster with 28 atoms, a third layer with 6 atoms is introduced and then the size of this layer is increased to 12 atoms to yield the 34 atom cluster. The increase in binding energy indicates that the third layer is important. If a third layer needs to be considered, then second neighbors around the primary chemisorption size will also be required. This is effectively observed for the 40 metal atom cluster (which contains 6 more atoms in the first layer than the 34 metal atom cluster) since the binding energy still increases. For the 52 metal atom cluster, more atoms have been added in the second and third layers so that all layers have equivalent number of atoms. The 64 metal atom cluster has all the second neighbors in the first layer and some more atoms in the second layer. Convergence of the binding energy is finally obtained for these two largest clusters, since the binding energies only differ by a few kcal/mol. Increasing the number of 11 electron silver atoms from three to six in the primary chemisorption site decreases a little the binding

energy as indicated in Table 4b for the 28 and 52 atoms clusters. Such a decrease is expected since the 11 electron atoms describe better the electron repulsion between the adsorbate and the surface. The addition of more 11 electron atoms did not produce any significant change in the binding energy. Therefore, the 52 metal atom cluster with six 11 electron atoms around the primary chemisorption site (Fig. 2) was chosen as the best cluster.

Table 4a shows that the MP2 contribution to the total binding energy rapidly converges to a value of about 25 kcal/mol. Therefore most of the binding energy is obtained at the Hartree–Fock level while the MP2 contribution is less than 20% of the Hartree–Fock contribution. The MP2 contribution could not be calculated for clusters with more than 40 atoms. But since it converges much faster than the Hartree–Fock contribution, the value of 25 kcal/mol was used to estimate the binding energy for the 52 atom cluster.

For all the binding energies reported in Table 4 the geometry of free sulfate was used and it was kept fixed through all the calculations. In the next section we study the relaxation of sulfate on the surface and its contribution to the binding energy.

4. Adsorbate relaxation

We discuss in this section the results of sulfate geometry optimizations and we show that the way in which the adsorbate geometry changes can be rationalized in terms the conservation of bond order on metal surfaces.

In these calculations the metal atoms were kept fixed and the sulfate atoms were allowed to relax until the minimum energy was obtained. The calculations were performed in C_{3v} symmetry and were stopped when the forces on each of the sulfate atoms were less than 0.001 au. Table 5 contains the results of a geometry optimization on a 52 silver atom cluster (see Fig. 3) for a non-eclipsed coordinated sulfate. The geometries for other sulfate coordinations have been reported in [39]. The last column in Table 5 corresponds to the geometric parameters of free sulfate and were obtained optimizing its geometry. The calculated S–O distance of 1.494 Å for free sulfate is in agreement with the value of 1.49 Å reported in the literature [40]. The numbers in brackets indicate the percentage change in a given geometric parameter. Table 5 shows that the length of the bond between the sulfur atom and the oxygens coordinated to the surface increases while the sulfur-uncoordinated oxygen bond length decreases. This is clearly and indication of the conservation of bond order on metal surfaces [30,41–43]. As the surface bond forms between the metal and the coordinated oxygens, the bond between these oxygens and the sulfur atom weakens and consequently the $S–O_{coord}$ distance increases. As a consequence of the weakening of the bonding between sulfur and the coordinated oxygens, the $S–O_{uncoord}$ bond strengthens and its bond length decreases. The tetrahedral angle of 109.5° of free sulfate is also distorted to yield a $O_{uncoord}–S–O_{coord}$ angle of 113.16°.

Table 5
Sulfate geometrical parameters obtained after a geometry optimization. Numbers in bracket indicate percentage change

	Adsorbed SO_4^{2-}	Free SO_4^{2-}
d ($S–O_{coord}$) (Å)	1.502 (0.54%)	1.494
d ($S–O_{uncoord}$) (Å)	1.446 (−3.21%)	1.494
Angle ($O_{uncoord}–S–O_{coord}$) (deg)	112.6 (2.80%)	109.5
d (O_{coord}–surface) (Å)	2.274	—

The strengthening and weakening of bonds is clearly seen in electron density difference maps between the electron density of adsorbed sulfate and that of free sulfate. Fig. 4 shows an electron density difference plot corresponding to the plane which contains the O–S–O fragment. The labels in the figure indicate which is the coordinated and the non-coordinated oxygen. The figure shows that there is a region of charge

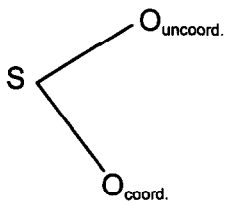

Fig. 4. Electron density difference map for adsorbed sulfate in the plane containing the O–S–O fragment. Note the depletion of charge between the sulfur atom and the coordinated oxygen atom. and the accumulation of charge between the sulfur and the uncoordinated oxygen atom.

accumulation between the sulfur atom and the noncoordinated oxygen atom. This charge accumulation is responsible for the strengthening of this bond after adsorption which in turn produces a decrease of 2.61% (see Table 5) of its bond length. On the other hand, a wide region of charge depletion is observed between the $S-O_{coord}$ bond which is responsible for the weakening and enlargement of 2.68% (Table 5) of this bond. Fig. 3 also shows a net accumulation of charge around the sulfur atom while around the oxygen atoms there are regions of charge accumulation and charge depletion which on average produce a decrease of the electron density around these atoms.

5. Nature of the adsorbate and charge transfer

Based on the thermodynamic and quantum chemical calculations of the previous sections, we discuss here the nature of the ionic adsorbate and the implications that this has in the modeling of surface reactions in the field of catalysis.

The adsorption of a single adsorbate will not change the work function of a metal. This is the justification for using the work function of the metal when one electron is added or subtracted (Fig. 1, first step of path A). Therefore, from the comparison of Eqs. (1) and (3) for the cation we obtain the result that

$$Q_{neutral} = Q^{+}_{neutral}$$

and from similar considerations for the anion we obtain that

$$Q_{neutral} = Q^{-}_{neutral}$$

The fact that the enthalpy change for the three processes in which a neutral species is adsorbed on (1) a neutral metal, (2) a positively charged metal and (3) a negatively charged metal is the same, implies that the final state of the adsorbate is the same in all cases. That is, once a proton, a hydride or a neutral hydrogen atom are adsorbed on a surface, they are the same species and they all look the same. This means, for example, that a proton adsorbed on a surface will have the same vibrational frequency, equilibrium distance, etc. as an adsorbed hydrogen atom or hydride anion. Depending on the nature of the adsorbate, the adsorbed species may look more like the neutral, the anion or the cation. This fact will mostly depend on the electron affinity of the adsorbate and that of the surface. For example, ab initio calculations indicate that there is a charge transfer of approximately one electron from the metal to the adsorbate in the case of F, Cl and Br adsorbed on the Ag(111) surface [44]. Therefore, we expect that adsorbed chloride ion will not loose any appreciable charge and adsorbed chlorine cation (Cl^{+}) will gain about two electrons from the surface, so that they all look the same on the surface. This is consistent with the notion that the excess charge present is infinitely delocalized over the infinite bulk. However, it is important to remark that these conclusions are only valid for metals which have no band gaps.

The fact that $Q_{neutral} = Q^{-}_{neutral} = Q^{+}_{neutral}$ has been tested in the literature with high quality ab initio calculations although attention was not called to this fact. Siegbahn and Wahlgren [34] have shown with high quality ab initio calculations that the addition of a single electron to large clusters of nickel atoms has little effect on the binding energy of atomic oxygen to the nickel surface.

The above thermodynamic cycles are valid

for polyatomic adsorbates as well as monoatomic adsorbates. In the case of monoatomic adsorbates the surface binding site is usually not in question, and the binding energy, Q, is well defined and measurable. However, for polyatomic adsorbates there are often practical difficulties such as several possible coordination modes and binding sites. Nevertheless, there will be a 'ground state' or lowest energy state for the adsorbate–surface system in terms of which a unique binding energy can be defined. The above thermodynamic cycles tacitly assume that the neutral gas phase species forms a stable adsorbate and this does not have to be the case. For specie having more than one unit of charge, Eqs. (1)–(4) need to be modified accordingly. In the case of a di-ion, for example, this would involve the approximation that the first and second ionization potential and or electron affinity of the bulk metal are the same and equal to the work function. This is probably a good approximation. The thermodynamic cycles are also valid for binding sites and coordination modes other than the preferred ones, but this complicates the definition of the binding energy.

The conclusions we have reached concerning the nature of adsorbed species based on thermodynamic arguments, represent conditions to which quantum mechanical results should conform, provided adequate clusters representing the metal surface are employed in the calculations. In the case of the hydrogen ion and the sulfate ion we have already investigated the quality of the clusters with respect to binding energies. We now investigate weather the cation, neutral and anion of a given species are all the same species on the surface of different clusters, as is predicted by our thermodynamic analysis. In order to judge if different adsorbates effectively correspond to the same species we will use adsorbate properties such as geometry and atomic charges based on Mulliken population analysis. We will use H^+ and H^- as monoatomic ions and OH^+ and OH^- as polyatomic ions.

Table 6
Proton and hydride charges obtained on clusters of different size

Cluster	H^+	H^-
4 (3, 1)	1.34	1.27
10 (7, 3)	1.34	1.27
16 (7, 6, 3)	1.20	1.21
34 (12, 10, 12)	1.22	1.23
82 (21, 19, 21, 21)	1.15	1.14

Table 6 contains the Mulliken populations for the proton and the hydride adsorbed on clusters of different size. In the case of the hydride, as the cluster size increases, more electrons are transferred to the metal. This is one of the reasons why large clusters are needed to obtain reliable binding energies: the cluster has the task of delocalizing the ion charge which is not possible in the case of small clusters. The hydrogen populations on the larger clusters are nearly the same for the adsorbed proton and hydride. This value corresponding to the effective charge of -0.2 is the same as the Mulliken population of adsorbed neutral hydrogen. Therefore, the large clusters also adequately describe the correct nature of the adsorbates as expected from the thermodynamics. In this case, the adsorbed proton and hydride look like neutral hydrogen. However the adsorbed ions do not necessarily have to look like the gas phase neutral specie because the neutral specie do not necessarily remain neutral after adsorption. Below we will give an example in which the gas phase neutral specie after adsorption became substantially ionic. For the H^+ and the H^- we also obtained the same perpendicular equilibrium distance above the surface of 2.0 bohr, which is the same value we obtain for the neutral H atom. Thus we see that the cation, neutral and anion adsorption are just different routes to the same final surface adsorbate. Because the cation has such a high binding energy (255 kcal/mol), it is tempting to believe that the cation should significantly reconstruct the surface or that the surface relaxation energy would contribute a significant amount to the overall binding energy. However, we have

Table 7
Oxygen and hydrogen populations for (A) free and (B) adsorbed OH species

	O	H	Electrons	Δe
(A) Free				
OH^+	7.588	0.412	8	
OH	8.389	0.611	9	
OH^-	9.185	0.815	10	
(B) Adsorbed				
OH^+	9.084	0.578	9.662	1.662
OH	9.060	0.602	9.662	0.662
OH^-	9.067	0.603	9.670	−0.330

shown that the adsorbed hydrogen ions are identical to adsorbed hydrogen atom. In this picture one expects that the amount of surface relaxation accompanying the cation or anion adsorption is just the same as that accompanying the adsorption of neutral hydrogen.

Table 7 contains the oxygen and hydrogen Mulliken populations for free and adsorbed OH^+, OH and OH^- calculated on a 28 atom cluster (12/10/6 atoms in the first, second and third layer). Besides the Mulliken populations Table 7 also indicates the number of electrons of the different OH species. In the case of the adsorbed species, Δe is the difference in the number of electrons of the adsorbed species minus the number of electrons of the free species. Once again, Table 7b shows that while OH^+ and OH gain 1.66 and 0.66 electrons from the surface, OH^- loses 0.33 electrons and finally adsorbed OH^+, OH and OH^- are the same adsorbate since they all have the same number of electrons and nearly identical O and H Mulliken populations. Whereas the adsorbed hydride resembles the neutral H atom, the adsorbed OH resembles more an hydroxide ion. From the geometry optimizations we obtained, for example, the same surface–oxygen distance (in a hollow site) of 3.08 bohr. In fact, we carried out the first geometry optimization for OH^+ and we then used this geometry as a starting point in the geometry optimizations of OH and OH^-. In this way, we obtained negligible forces on OH and OH^-, further proving that they are effectively the same adsorbate. As Table 7 shows, on the 28 atom cluster the hydroxyl anion loses 0.33 electrons towards the surface. We also repeated this calculation on a 52 atom cluster and found in this case that hydroxyl loses 0.34 electrons. Thus, essentially the same charge transfer is obtained by doubling the size of the cluster, which is indicative that convergence with cluster size has been achieved.

The binding energy of OH^- can be calculated with Eq. (2). The work function of silver is 109 kcal/mol [31] and the electron affinity of

Table 8
Charge transfer upon chemisorption of sulfate. Negative numbers indicate that charge is transferred to the surface. The designation of eclipsed refers to the relative position of the three oxygen contact atoms to metal atoms of the three-fold site

		22 12, 10	28 12, 10, 6	34 12, 10, 12	40 18, 10, 12	52 18, 19, 15	64 27, 25, 12
Eclipsed	S	0.010	0.0	−0.008	0.018	0.004	0.009
	O(coord)	−0.093	−0.091	−0.088	−0.101	−0.095	−0.098
	O(uncoord)	−0.122	−0.122	−0.123	−0.142	−0.143	−0.144
	total	−0.391	−0.395	−0.395	−0.427	−0.424	−0.429
Non − eclipsed	S	0.039	0.029	0.027	0.017	0.031	0.039
	O(coord)	−0.080	−0.076	−0.074	−0.072	−0.076	−0.079
	O(uncoord)	−0.126	−0.126	−0.127	−0.138	−0.154	−0.153
	total	−0.327	−0.325	−0.322	−0.0337	−0.351	−0.351
Monocoord.	S	−0.033	−0.033	−0.033	−0.028	−0.018	−0.019
	O(coord)	0.051	0.064	0.031	0.033	0.055	0.059
	O(uncoord)	−0.091	−0.098	−0.089	−0.094	−0.105	−0.106
	total	−0.255	−0.263	−0.269	−0.277	−0.278	−0.278

OH radical is −42 kcal/mol [31]. The binding energy of a single OH radical can be calculated according to the BOC-MP formula [30]:

$$Q_{OH} = \frac{Q_O^2}{Q_O + D} \quad (5)$$

where Q_O is the binding energy of oxygen on silver (which is 80 kcal/mol [41]) and D is the energy of the O–H bond in the gas phase (102 kcal/mol [31]). From Eq. (5) we obtain a binding energy of 35 kcal/mol for OH radical. Therefore, the binding energy of OH^- is 102 kcal/mol according to Eq. (2). In order to check the reliability of our ab initio calculations, we also calculated the OH binding energy on a 52 atom cluster (Fig. 3). We obtained a value of 108 kcal/mol (91 kcal/mol at the SCF level and 17 kcal/mol at the MP2 level of theory) which is in very good agreement with the value obtained from Eq. (2). As in the case of the hydrogen ions, most of the binding energy for OH is obtained at the Hartree Fock level of theory.

Table 8 contains the difference between the charge of free sulfate and the charge of adsorbed sulfate calculated on clusters of different size. The numbers in the top row indicate the total number of silver atoms in the cluster modeling the Ag(111) surface and the second row indicates the number of silver atoms in each layer of the cluster. The negative numbers indicate that electron density is transferred to the surface. Our calculations indicate that about 0.4 electron is transferred to the surface upon sulfate chemisorption. In the case of bisulfate, Bockris [6] has obtained a charge transfer of 0.2 electrons. Therefore, the fact that we obtain twice that charge transfer for a similar anion which has twice the charge of bisulfate is reasonable. These results indicate that adsorbed sulfate will remain in the anionic form and will not be very different from free sulfate. In the case of SO_3, we observed essentially no charge transfer indicating that the adsorbed species in this case looks like the neutral. Therefore, its anion, SO_3^{2-}, should lose about two electrons to the surface. Our calculations show that SO_3^{2-} loses increasingly more charge to the surface as the size of the cluster increases. We obtained a binding energy of 205 kcal/mol on the 52 atom cluster which we consider to be a lower limit and is not a converged value. The fact that a higher binding energy than that of SO_4^{2-} is obtained for SO_3^{2-} is consistent with the larger charge transfer of SO_3^{2-}.

In the chemistry of sulfur oxides on metal surfaces, sulfur oxide specie containing three and four oxygen atoms have been proposed to exist at elevated temperatures on several metal surfaces on the basis of experimental data [45–48]. For example, on the Ag(110), an SO_4 species exits at high temperatures in the 500–873 K range [47]. We believe that the SO_4 specie observed at high temperatures is sulfate. The decomposition of sulfate to yield either SO_3(ad) + O(ad) or SO_2(gas) + O_2(ad) will only occur at high temperatures since these reactions are very endothermic [38]. The enthalpy change of first decomposition path is $\Delta H = +84$ kcal/mol + $(X - 2\phi)$) on the Ag(111) surface, where X is the energy required to remove both anion electrons from sulfate, and, 2ϕ is the energy required to remove two electrons from the metal surface. Since we have shown that there is a small amount of electron transfer from sulfate to the surface, the quantity $(X - 2\phi)$) should be slightly negative. Therefore we estimate that the decomposition of sulfate is significantly endothermic, certainly $\Delta H > 50$ kcal/mol. For the second path, the enthalpy is greater than that of the first path by 25 kcal/mol. This means that sulfate on Ag(111) should be a stable adsorbate at elevated temperatures, but, should decompose before the desorption barrier of 160 kcal/mol could be overcome. The resultant SO_3 produced by decomposition of sulfate along the first path will readily decompose to SO_2 and O since this reaction has a low activation barrier of 10 kcal/mol [38]. Regardless of the path, the result is always that sulfate decomposition at elevated temperatures ultimately

leads to SO_2 desorption, as it is observed experimentally, see Ref. [38] and references therein. In the case of sulfur trioxide, Outka et al. [47] did not observe an ionic SO_3 surface species. The observed SO_3 vibrational spectrum was unlike that of ionic sulfites [47]. This is also in agreement with our results which predict that adsorbed SO_3 will look like the neutral and not like the sulfite anion.

The result that the final adsorbate is the same, in the zero coverage limit, regardless of the charge of the incoming adspecie has the consequence that reactions between adsorbed 'ions' will have essentially the same activation barriers, relative to adsorbed reactants, as does the reaction between the neutral species. For example, the reaction at very low coverages between adsorbed H^+ and OH^- will have the same barrier as the reaction between adsorbed H and OH. The activation barrier of the surface reaction relative to gas phase (ionic) reactants will be different but it will be the same relative to adsorbed reactants. Therefore, in the prediction of activation barriers of surface reactions relative to surface adsorbed reactants based on the bond order conservation-morse potential (BOC-MP) method of Shustorovich, one should just use the heats of adsorption of the neutral specie in the BOC-MP formulas [30].

6. Conclusions

The nature of chemisorbed ions has been investigated both from a thermodynamic and quantum chemical point of view. The cation, the anion or the neutral are the same entity once adsorbed on the surface. The adsorbed species may resemble the anion, the cation or the neutral depending on the relative electron affinities and/or ionization potentials of the metal and the adsorbate. A proton, for example, gains 1.2 electrons on the surface while hydride loses 0.8 electrons and thus the adsorbed species resembles adsorbed neutral hydrogen which has 1.2 electrons ($H^{-0.2}$). On the other hand, OH^+ gains 1.66 electrons, OH gains 0.66 electrons and OH^- only loses 0.33 electrons and in this case the adsorbed species $OH^{-0.67}$ resembles the anion. For the sulfur oxides we found that the adsorbed tetraoxide resembles sulfate which is in agreement with its stability at high temperatures [47]. The adsorbed sulfur trioxide, on the other hand, should be very much like the neutral.

Ions may bind more or less strongly than the neutral depending on the difference between the ionization potential (electron affinity) of the neutral and the work function of the metal. For example, in the case of platinum, the cations of alkali metals are less strongly bound than the neutral atoms while the halides show increases in binding energy as compared to neutral halogens in the range of 25–60 kcal/mol. Li^+ and Na^+ have binding energies that are greater than those of the neutrals by 15 and 9 kcal/mol respectively, but K^+ is less strongly bonded by 9 kcal/mol than atomic potassium [49].

Larger clusters are required for ions than for neutral species before convergence of binding energy with cluster size can be achieved. We attribute this to the fact that the cluster model of the surface has the task of delocalizing the electric charge which the smaller clusters do not do as well. Most of the binding energy of the close shell ions we examined is obtained at the Hartree–Fock level of theory.

Acknowledgements

We thank the American Science Materials Technologies Inc. for support of this work. H.L.S. thanks the National Science Foundation for the South Dakota EPSCoR grant (NSF Grant No. EHR-9108773), the State of South Dakota Future Fund and the IBM Corporation for partial support of this project. E.M.P. thanks the Consejo Nacional de Investigaciones Cientificas y Técnicas (CONICET) de la República Argentina for the fellowship granted.

References

[1] E. Herrero, K. Franaszczuk and A. Wieckowski, J. Phys. Chem. 98 (1994) 5074.
[2] Z. Shi, J. Lipkowski, M. Gamboa, P. Zelenay and A. Wieckowski, J. Electroanal. Chem. 366 (1994) 317.
[3] C. Chen, S.M. Vesecky and A.A. Gewirth, J. Am. Chem. Soc. 114 (1992) 451.
[4] M.S. Zei, D. Scherson, G. Lehmpfuhl and D.M. Kolb, J. Electroanal. Chem. 229 (1987) 99.
[5] P.W. Faguy, N. Markovic, R.R. Adzic, C.A. Fierro and E.B. Yeager, J. Electroanal. Chem. 289 (1990) 245.
[6] J. O'M. Bockris, M.G. Gamboa-Aldeco and M. Szklarczyk, J. Electroanal. Chem. 339 (1992) 355.
[7] P. Zelenay and A. Wieckowski, J. Electrochem. Soc. 139 (1992) 2552.
[8] Mrozek, M. Han, Y.-E. Sung and A. Wieckowski, Surf Sci. 319 (1994) 21.
[9] O.M. Magnussen, J. Hagebock, J. Hotlos and R.J. Behm, Faraday Discuss. 94 (1992) 329.
[10] X. Gao, G.J. Edens and M.J. Weaver, J. Electroanal. Chem. 376 (1994) 21.
[11] G.J. Edens, X. Gao and M.J. Weaver, J. Electroanal. Chem. 375 (1994) 357.
[12] L. Wan, S. Yan and K. Itaya, J. Phys. Chem. 99 (1995) 9507.
[13] F.C. Nart and T. Iwasita, J. Electroanal. Chem. 308 (1991) 277.
[14] F.C. Nart and T. Iwasita, Electrochim. Acta 37 (1992) 2179.
[15] F.C. Nart and T. Iwasita, J. Electroanal. Chem. 322 (1992) 289.
[16] F.C. Nart, T. Iwasita and M. Weber, Electrochim. Acta 39 (1994) 961.
[17] F.C. Nart, T. Iwasita and M. Weber, Electrochim. Acta 39 (1994) 2093.
[18] T. Iwasita, F.C. Nart, A. Rodes, E. Pastor and M. Weber, Electrochim. Acta 40 (1995) 53.
[19] K. Kunimatsu, M.G. Samant and H. Seki, J. Electroanal Chem. 258 (1989) 163.
[20] K. Kunimatsu, M.G. Samant and H. Seki, J. Electroanal. Chem. 272 (1989) 185.
[21] M.G. Samant, K. Kunimatsu, H. Seki and M.R. Philpott, J. Electroanal. Chem. 280 (1990) 391.
[22] D.B. Parry, M.G. Samant, H. Seki, M.R. Philpott and K. Ashley, Langmuir 9 (1993) 1878.
[23] Y. Shingaya and M. Ito, J. Electroanal. Chem. 372 (1994) 283.
[24] F.C. Nart and T. Iwasita, Electrochim. Acta 37 (1992) 385.
[25] A. Rodes, E. Pastor and T. Iwasita, J. Electroanal. Chem. 369 (1994) 183.
[26] T. Iwasita, A. Rodes and E. Pastor, J. Electroanal. Chem. 383 (1995) 181.
[27] A. Rodes, E. Pastor and T. Iwasita, J. Electroanal. Chem. 376 (1994) 109.
[28] G.A. Somorjai, Introduction to Surface Chemistry and Catalysis, Wiley, New York, 1994.
[29] Y. Guang, J.A. Marcos, G.W. Simmons and K. Klier, J. Phys. Chem. 94 (1990) 7597.
[30] E. Shustorovich, Adv. Catal. 37 (1990) 101.
[31] R.C. Weast (Ed.), CRC Handbook of chemistry and Physics, 62nd Ed., Chemical Rubber, Boca Raton, 1982.
[32] I. Panas, J. Schule, P. Siegbahn and U. Wahlgren, Chem. Phys. Lett. 149 (1988) 265.
[33] P.E.M. Siegbahn, L.G.M. Pettersson and U. Wahlgren, J. Chem. Phys. 94 (1991) 4024.
[34] P.E.M. Siegbahn and U. Wahlgren, Int. J. Quantum Chem. 42 (1992) 1149.
[35] S. Huzinaga, M. Klubokowski and Y. Sakai, J. Phys. Chem. 88 (1984) 4880.
[36] J. Andzelm, S. Huzinaga, M. Klubokowski and E. Radzio, Mol. Phys. 52 (1984) 1495.
[37] S. Huzinaga, L. Seijo, Z. Barandiaran and M. Klubokowski, J. Chem. Phys. 86 (1987) 2132.
[38] H. Sellers and E. Shustorovich, Surf Sci. 346 (1996) 322.
[39] E.M. Patrito, P. Paredes Olivera and H. Sellers, J. Phys. Chem., submitted.
[40] A.F. Wells, in: Structural Inorganic Chemistry, 5th Ed., Clarendon Press, Oxford, 1984.
[41] E. Shustorovich, Surf Sci. Rep. 6 (1986) 1.
[42] H.L. Sellers, in: H.L. Sellers and J.T. Golab (Eds.), Theoretical and Computational Approaches to Interface Phenomena, Plenum Press, New York, 1994.
[43] E. Shustorovich, in: E. Shustorovich (Ed.), Metal-Surface Reaction Energetics, VHC, New York, 1991.
[44] P.S. Bagus, G. Pacchioni and M.R. Philpott, J. Chem. Phys. 90 (1989) 4287.
[45] St. Astegger and E. Bechtold, Surf Sci. 122 (1982) 491.
[46] M.L. Burke and R.J. Madix, Surf Sci. 194 (1988) 223.
[47] D.A. Outka, R.J. Madix, G.B. Fisher and C. DiMaggio, J. Phys. Chem. 90 (1986) 4051.
[48] Y.-M. Sun, D. Sloan, D.J. Alberas, M. Kovar, Z.-J. Sun and J.M. White, Surf Sci. 319 (1994) 34.
[49] H. Sellers, E.M. Patrito and P. Paredes Olivera, Surf Sci., in press.